LWT - Food Science and Technology 251 (2026) 119532

Contents lists available at ScienceDirect

LWT

journal homepage: www.elsevier.com/locate/lwt

Novel biodegradable antimicrobial film and its suitability as food contact material against *Campylobacter* spp.

Laura Aguerri [a,b], Estela Pérez-Bondía [a], Silvia Lóbez [a], Frédéric Leonardi [b], Filomena Silva [a,c,d,*]

[a] *I3A – Aragon Institute of Engineering Research, University of Zaragoza, 50018, Zaragoza, Spain*
[b] *IPREM, CNRS, UPPA, Université de Pau et des Pays de l'Adour, Pau, France*
[c] *ARAID – Agencia Aragonesa para la Investigación y el Desarrollo, 50018, Zaragoza, Spain*
[d] *Faculty of Veterinary Medicine, University of Zaragoza, 50013, Zaragoza, Spain*

ARTICLE INFO

Keywords:
Biodegradable polymers
Benzyl isothiocyanate
Active packaging
anti-*Campylobacter* material
Migration

ABSTRACT

Our study focused on developing biodegradable active films with antibacterial properties against pathogenic *Campylobacter* spp. For that purpose, an inclusion complex (IC) synthesized with β-cyclodextrin and benzyl isothiocyanate (BITC) was incorporated by extrusion into polyhydroxybutyrate (PHB) and polylactic acid (PLA), at 2.5 and 5 %, and films were prepared by hot-pressing. The anti-*Campylobacter* effect was assessed by direct contact and in vapour phase. The IC alone exhibited strong antibacterial activity comparable to pure BITC. PHB_IC films showed good antibacterial performance, achieving total inhibition of *C. jejuni* at 2.5 % and *C. coli* at 5 %, and yielding inhibition halos up to 50 mm in vapour phase. Contrarily, PLA_IC films showed no antibacterial effect, and BITC was not detected, likely due to differences in polymer matrix or extrusion conditions. To further investigate the use of these films as food contact materials, migration tests into food simulants were conducted. Volatile and non-volatile compounds were identified by GC-MS and UPLC-QTOF-MS, with most being intentionally added and only three detected as non-intentionally added substances. Overall, the developed PHB-based material showed strong anti-*Campylobacter* spp., no detectable migrants from the IC, and industrial scalability, supporting its potential for active food packaging, although further studies are needed.

1. Introduction

Among all foodborne pathogens, *Campylobacter* spp., a gram-negative non spore forming bacteria, is a major threat to public health across the world, being the most common bacterial cause of gastroenteritis (EFSA, 2024a; WHO, 2020). In fact, *Campylobacter* was the most reported pathogen in the European Union (EU) in 2023, causing 148, 181 cases of illness, 12,194 hospitalizations and 44 deaths (EFSA & ECDC, 2024), although these numbers are believed to be underestimated, and the actual number of infections would be closer to nine million each year (EFSA, 2024b). Furthermore, their associated economical costs are estimated to be €2.4 billion each year (EFSA, 2024b).

Campylobacteriosis, the infection caused by this pathogen, usually results in fever, diarrhoea and abdominal cramps and lasts up to 10 days (EFSA, 2024a; WHO, 2020). *Campylobacter jejuni* and *Campylobacter coli* are the most relevant species, being responsible for almost 95 % of *Campylobacter*-associated infections (EFSA, 2024a). Due to its faecal -intestinal- origin from different bird species (Abulreesh et al., 2017), the top food vehicles implied in *Campylobacter* transmission are those of animal origin, such as broiler or turkey meat and eggs, but it can also contaminate other products like non-treated water, milk, or mixed foods, with the ability to survive to extended periods of refrigeration and freezing (EFSA, 2024a). To ensure its control, different strategies are being developed with an emphasis on antimicrobial active packaging, which incorporate substances in the packaging material that interact with the food or the atmosphere inside the packaging to delay or inhibit microbial growth (Sofi et al., 2018). Among the wide variety of antimicrobials used, those volatile compounds derived from plants are the most explored due to their natural origin and broad range of antimicrobial effects (Gniewosz et al., 2022; Manso et al., 2015; Mukurumbira et al., 2022; Silva et al., 2018).

Isothiocyanates, such as allyl isothiocyanate (AITC) or benzyl isothiocyanate (BITC), are bioactive compounds predominantly derived

* Corresponding author. Departamento de Química, Facultad de Veterinaria, Calle de Miguel Servet, 177, 50013, Zaragoza, Spain.
E-mail address: filomena@unizar.es (F. Silva).

https://doi.org/10.1016/j.lwt.2026.119532
Received 16 June 2025; Received in revised form 17 March 2026; Accepted 16 May 2026
Available online 17 May 2026

from Brassicaceae vegetables and herbs (Hoch et al., 2024). These compounds are of special interest due to their broad antimicrobial properties (Luciano & Holley, 2009; Sun et al., 2021; Wilson et al., 2013; Yadav et al., 2022), including gram-negative bacteria (Nowicki et al., 2021). In the food industry, some isothiocyanates are primarily used as flavouring agents. This is the case of BITC, a substance classified as Generally Recognised as Safe in the U.S. (Waddell et al., 2007), listed as food flavouring in the EU under Commission implementing Regulation (EU) 872/2012, and used to impart mustard-like scents. However, some limitations of their use are their high volatility and non-water solubility, which hinders their incorporation into packaging materials (Jiang et al., 2022). To overcome these drawbacks, encapsulation strategies such as the formation of inclusion complexes with cyclodextrins are being explored to enhance their compatibility with the polymer matrix and reduce their volatility (Li et al., 2022; Wu et al., 2022). These complexes retain the active compounds at the molecular level, improving thermal stability and solubility, enabling controlled release and minimizing losses during processing, outperforming conventional incorporation methods such as direct blending (Capelezzo et al., 2018; Perinelli et al., 2020; Xiao et al., 2021).

Due to the environmental impact of petroleum-based plastic packaging, biodegradable and/or compostable polymers, such as polylactic acid (PLA) and polyhydroxybutyrate (PHB) are nowadays preferred when designing active packaging materials (Manzoor et al., 2023; Mittal et al., 2023; Rusková et al., 2023; Taktak et al., 2024). Furthermore, although many studies are based on developing novel active food materials with different properties, most of them use laboratory-scale techniques such as solvent casting (Ma et al., 2018; Zhuikova et al., 2022) and do not address the chemical risks of those novel materials, which is of mandatory compliance in the EU for all food contact materials (FCM) following Regulation EC 10/2011 (Commission Regulation (EU) No 10/2011), and Regulation 450/2009 (Commission Regulation (EC) No 450/2009) specific for active and intelligent packaging, meaning that neither their chemical safety, nor their feasibility of scale-up and use as commercial food packages have been thought-through, all of which hinders their transfer process into the industry.

The goal of our research was to develop an active biodegradable material containing BITC complexed with β-cyclodextrin (β-CD) that was effective against *Campylobacter* spp. and could be produced by industrially sclalable methods, while addressing active material safety as food contact material according to the existing EU regulation.

2. Materials and methods

2.1. Materials

For the synthesis of the inclusion complex (IC), β-cyclodextrin (β-CD) was provided by Roquette (Lestrem, France) and benzyl isothiocyanate (BITC; 98% purity) was supplied by Thermo Scientific (Waltham, USA). For film preparation, two commercial polymers in the form of pellets were used: Polylactic acid (PLA) (PLE 005-A, NaturePlast, France) and the commercial product BIO-FED GP1045 (M·VERA®, Germany) was used as poly(3-hydroxybutyrate) (PHB), after confirmation by NMR-H analysis. Ethanol, hexane, and dimethyl sulfoxide (DMSO) were provided by PanReac (Spain).

2.2. Methods

2.2.1. Synthesis of inclusion complex

The inclusion complex (IC) was prepared following a precipitation method described in Petrovic et al. (2010) with slight modifications. Briefly, 25 g of β-CD were added into 250 mL ethanol/water (1:2 v/v) and magnetically stirred at 55 °C until completely dissolution. Then, 6.25 g of BITC were dissolved in 50 mL of ethanol (10 % w/v) and slowly added to the β-CD solution. The mixture was continuously stirred for 30 min at 55 °C and a precipitate was formed. After this time, the mixture was removed from the heating bath and stirring was maintained for another 4h at room temperature. The final solution was refrigerated overnight. The cold precipitated material was recovered by vacuum filtration and kept at −80 °C until freeze-drying. The freeze-dried BITC-β-CD IC was stored at 6 °C until further use.

2.2.2. Films development

2.2.2.1. Masterbatch preparation. IC polymer masterbatches containing a mixture of either PHB or PLA and IC were prepared by extrusion using a 16 mm co-rotating twin-screw extruder (LabTech Engineering Company Ltd, Thailand) following a two-step extrusion procedure. Firstly, each polymer blend was prepared by extruding the commercial product (pellets) previously dried (overnight at 70 °C) to reduce moisture. Information on extrusion conditions for each polymer can be found in Supplementary Information (Table S1). The polymer filament obtained (2 mm diameter) was pelletized in 1 mm-length pellets. After drying the pellets at 70 °C for 6 h, masterbatches were prepared by adding IC (powder) at 15% (w/w) to the extruded blend, followed by homogenization, extrusion and pelletizing in the same way as described above.

2.2.2.2. Dilution and films preparation. Dried pellets (masterbatches and polymer pellets) were used to prepare dilutions at two different concentrations of IC in the polymer matrix (2.5 and 5% (w/w), named _2.5IC and _5IC respectively) by the same extrusion process as with the masterbatches (section 2.3.2). Once the pellets of each diluted sample were dried, they were used to prepare different films (150 μm thickness) using a hydraulic hot-pressing machine (Darragon, France). For each film, 4 g of pellets were disposed in between two steel plates which were set in the hot-pressing machine. The thermopressing cycle consisted of 3 min at 175 °C with no pressure to ensure complete melting, followed by 2.5 min of pressure (two hundred bar) and then cooling at room temperature without pressure. After that, films were placed inside aluminium thermo-sealed bags and stored at −20 °C. Apart from the films containing IC, control films without any added compound (0IC) were developed from commercial pellets extruded and pelletized, and films were prepared in the same conditions as already described for the IC-containing films.

2.2.3. Materials characterization

Material thermal analysis was performed by thermogravimetric analysis (TGA) and differential scanning calorimetry (DSC). TGA was performed on approximately 10 mg of each sample without any further preparation using a thermal analyser TGA 4000 (Perkin, USA). TGA was operated with a heating ramp (10 °C/min) from 30 to 650 °C on air. DSC was performed on films using a DSC Q-100 instrument (TA Instruments, USA). Approximately 10 mg of film samples were placed on aluminium pans, sealed, and introduced in the instrument. Then, DSC instrument was equilibrated at 0 °C and an initial temperature heating-cooling cycle was set (ramp 10 °C per minute up to 190 °C) to remove sample's previous thermal history. After removing the material's thermal history, samples were subjected to a second heating cycle from 0 to 190 °C at a heating rate of 10 °C per minute. An empty sealed aluminium pan served as reference and all measurements were conducted under nitrogen atmosphere (50 mL per minute flow rate). Second heating ramp was used for determining the melting temperature (T_m) and the fusion enthalpy (ΔH_m), and the degree of crystallization (χ_c) was calculated as described by Garcia-Garcia et al. (2016) following Equation (1):

Equation (1):

$$\chi_c\ (\%) = 100 \cdot [\Delta H_m\ /\ (\Delta H_0 \cdot \Delta w)]$$

where ΔH_0 is the theoretical fusion enthalpy value of the polymer with a degree of100% crystallinity. For PHB, this value corresponds to 146.0 J/g for PHB (Arrieta et al., 2014) and 93.0 J/g for PLA (Battegazzore et al.,

2011). Δw represents the weight fraction of the polymer in each blend.

Besides thermal analysis, X-ray diffraction analysis (XRD), Fourier-transformed infrared spectroscopy (FT-IR) and Scanning electron microscopy (SEM) were also performed directly on film samples. XRD patterns were obtained with an XRD PANalytical Empyream (Malvern Panalytical, United Kingdom) diffractometer system equipped with copper as anode material (generator system of 45 kV voltage and 40 mA current). The diffractograms were recorded in the 2θ angle range between 10 and 90°. The system operated at 25 °C, in continuous scan mode, with a step size of 0.0130° and a scan step time of 143.82 s. FT-IR was obtained using Spectrum One instrument (PerkinElmer, USA) in the wavelength range of 4000 to 650 cm^{-1}. SEM (Inspect F50, 15 kV) was used to evaluate surface and cross-sectional morphology of films. Prior to visualization, samples were coated with palladium. For cross-sectional imaging, they were also subjected to cryogenic fracture under nitrogen before visualization.

Film thickness was determined using a digital micrometre (Mitutoyo, Spain) directly on films, conducting five different measurements in randomly chosen places of the film for each sample.

2.2.4. Determination of BITC content in IC and active films

BITC content in the IC and in the films was determined by GC-MS after a solvent-solvent extraction according to Yuan et al. (2009) with some modifications. First, a calibration curve of BITC was prepared in sealed glass vials containing 0.01 g of β-CD and different concentrations of BITC. Then, equal volumes of hexane and water were added to the vials, and vials were closed and let for 2 h at room temperature in a balanced stirrer. Stirring time was chosen based on inhouse previous studies, which ensured that all BITC present in the sample migrated to the organic solvent. Then, the organic fraction was removed, diluted appropriately in hexane, and transferred to chromatography vials to be analysed by GC-MS. The quantification of BITC in the IC was determined by weighting 0.01 g of the complex followed by the extraction method described above. For BITC determination in active films, the method was slightly modified to ensure that all BITC embedded into the polymer matrix was quantified. For that reason, samples (2 cm × 0.5 cm) were placed in sealed vials containing distilled water, sealed, and let for 72 h at RT with balanced stirring, enhancing the migration of the complex, with a more hydrophilic nature, to the aqueous medium. After the incubation period, a liquid-liquid extraction was performed with hexane. An equal volume of hexane was added to the vials and balance-stirred for 2 h more at room temperature, so that BITC transferred to the organic fraction. Then, the appropriate dilution of the organic fraction was performed and analysed as described above. All the samples, IC, and polymer films were analysed by triplicate.

The final concentration of BITC in the calibration curve vials for GC-MS ranged from 1.19 to 12.90 μg/mL. BITC in liquid samples was quantified by GC-MS using direct injection (1 μL) with an automatic CombiPal injector in a GC 6890 N gas chromatographic system coupled to a 5975 Mass Spectrometry Detector (Agilent Technologies, USA). Chromatographic separation was performed on a Zebron ZB 624 column (30 m × 0.250 mm x 0.250 μm) column with a helium flux of 2.5-2.6 mL/min. Column temperature was set at 60 °C for 4 min, followed by a heating ramp (15 °C/min) up to 220 °C and held 2 min at that temperature. MS was operated on scan mode (45-450 m/z). After determining the BITC peak area of each calibration point (Supplementary Information, Fig. S1), sample analyses were carried out under the same conditions, and the resulting areas were interpolated against calibration curve to determine BITC concentrations. When necessary, samples were appropriately diluted prior to analysis to ensure they fell within the range of the calibration curve.

2.2.5. Antibacterial activity assays

2.2.5.1. Bacterial strains and growth conditions. For the antibacterial activity tests, *Campylobacter* reference strains *Campylobacter coli* ATCC 33559 (*C. coli*) and *Campylobacter jejuni* ATCC 33560 (*C. jejuni*) were used. A concentrated bacterial suspension of each strain was stored at –80 °C in Brain Heart Infusion broth supplemented with 20 % (v/v) glycerol. Before the assays, strains were defrosted and subcultured firstly in *Campylobacter* blood-free selective medium [modified CCDA – Preston (Oxoid, UK)] to ensure maximum purity, and secondly in Muller Hinton agar (MHA; Oxoid, UK) supplemented with 5 % defibrinated horse blood (Oxoid, UK). Cultures were grown at 37 °C for 48 h under microaerophilic conditions (6% O_2, 7.1% CO_2, 3.6% H_2, 83% N_2) in gas tight containers using an Anoxomat Culture System (Advanced Instruments, UK). Then, grown colonies were used to prepare bacterial suspensions in 0.9 % NaCl. For inoculum preparation, these suspensions were diluted until obtaining an absorbance at 600 nm (OD_{600}) of 0.1 (approximately 10^8 CFU/mL). After that, a 1:100 dilution of the inoculum was prepared in cation-adjusted MH broth supplemented with 5 % lysed horse blood (MH-F) to obtain a final inoculum concentration of 1×10^6 CFU/mL. Blood supplementation of broth was performed under Clinical Laboratory Standards Institute (CLSI) M45 guidelines for fastidious microorganisms, such as *Campylobacter* spp. (CLSI, 2016). Lysis of blood was performed following the M07-A9 CLSI guidelines (CLSI, 2012).

2.2.5.2. Antibacterial activity of BITC and IC. The antibacterial activity of pure BITC and IC was evaluated through broth macrodilution method according to the CLSI guidelines for antimicrobial susceptibility testing for fastidious bacteria (CLSI, 2016). First, solutions of pure BITC and IC (10 mg/mL) were prepared in DMSO. Then, several dilutions were performed in MH-F broth containing different concentrations of DMSO until obtaining final stocks solutions of 16 μg/mL BITC and 144 μg/mL IC. For Minimal Inhibitory Concentration (MIC) determination, serial dilutions of each antimicrobial were performed in test tubes and inoculated with equal volume of bacterial inoculum. Final concentrations of antimicrobials in tubes were in the range of (0.062-8 μg/mL BITC and 0.56-72 μg/mL IC), while final concentration of bacteria in each tube was 5×10^5 CFU/mL. DMSO concentration inside test tubes was in any case lower than 2 % (v/v). Furthermore, controls of pure β-CD in the same range of concentration as IC were included, as well as bacterial and broth growth controls containing the maximum amount of DMSO added. Test tubes were incubated for 48 h at 37 °C in microaerophilic conditions as described above. After the incubation period, MIC, defined as the minimum concentration of BITC or IC that prevented visible bacterial growth (CLSI, 2012), was determined. For Minimal Bactericidal Concentration (MBC), 20 μL of each tube were plated twice into blood agar plates, incubated again at 37 °C for 48h in microaerophilic conditions and observed for growth according to CLSI guidelines (CLSI, 1999). MBC was defined as the minimum concentration of antimicrobial that resulted in a 99.9% reduction of bacterial growth (less than 1 bacterial colonies). Three replicates for each experiment were used and at least three independent experiments were performed for each strain and antimicrobial used.

2.2.5.3. Antibacterial evaluation of films. The anti-*Campylobacter* effect of films was evaluated in both liquid and solid media against each bacterial strain. Before the tests, films were sterilised under UV light for 30 min on each side. For liquid media assay, film samples (2 × 0.5 cm) were placed in glass tubes and immersed in 1 mL of the inoculum (1×10^6 CFU/mL) of either *C. coli* or *C. jejuni*. Samples were kept at 37 °C for 48 h under microaerobic conditions and then the effect of the film on *Campylobacter* growth was determined in the same way as described for BITC and IC (section 2.6.1.2). Three replicates of each active and control films were used in each experiment, and at least three independent experiments were performed.

For the solid medium assay, blood agar plates were inoculated with 100 μL of the inoculum spread evenly on the surface of the agar and allowed to dry. Afterwards, 2 × 2 cm film samples (actives and controls)

were placed in the inner part of the Petri dish lid to ensure no direct contact with the inoculated agar and to allow only vapour phase diffusion of the volatile BITC from the active film to the Petri dish atmosphere and the agar surface. Petri dishes were incubated at 37 °C for 48 h under microaerophilic conditions. After incubation, inhibition zones (zones without visible bacterial colonies) were measured using a digital gauge (Comecta S.A., Spain). Three replicates of each film were used in each experiment, and at least three different independent experiments were performed for each strain and film.

For both antibacterial tests, control films without IC (PHB_0IC and PLA_0IC) as well as growth controls (without film) for each strain were also included in each experiment.

2.2.6. Evaluation of chemical safety (migration tests)

The assessment of the chemical safety of the films was performed following Regulation EC 10/2011 (Commission Regulation (EU) No 10/2011) guidelines into two different food simulants [simulant A - 10 % ethanol (v/v) as aqueous simulant and simulant D2 - 95 % ethanol (v/v) as fat simulant]. Migration experiments were conducted by immersing control and active film samples (6 dm^2/kg simulant) for 10 days at 20 °C into food simulants. After that time, samples were analysed for volatile and non-volatile substances by GC-MS and UPLC-QTOF MS, respectively. Samples containing only the simulants were defined as blanks and were used to make the positive identification of compounds originated only from film samples. All migration tests were conducted in triplicate.

2.2.6.1. Volatile substances. Chromatographic separation of volatile substances was performed using an GC 8860 (Agilent, USA) equipped with a coupled to a Mass Spectrometry Detector 5977C GC/MSD single quadrupole with automatic injector PAL RSI 85 (Agilent, USA). The extraction of volatiles was performed on HS-SPME-GC-MS with a divinylbenzene/carboxene/polydimethylsiloxane (DVD/CAR/PDMS) 57298-U fibre (Nitinol-core (NIT), 23 ga, 50 μm (DVB layer), 30 μm (CAR/PDMS layer)) provided by Supelco for use with autosampler. The chromatography parameters were set as follows: First, SPME extraction took place at 80 °C for 5 min with agitation. Fibre was desorbed for 2 min at the injector (250 °C) in splitless mode, and the helium flow was 1.2 mL/min. Oven temperature program was set at 50 °C (3 min), followed by heating ramps of 10 °C/min to 150 °C, 5 °C/min to 200 °C and 10 °C/min to 300 °C (2 min). MSD acquisition was performed in SCAN mode (45-450 m/z).

2.2.6.2. Non-volatile substances. Chromatographic separation was performed using an Acquity UPLC system from Waters Corporation (Milford, MA, USA) equipped with a UPLC BEH C18 column (1.7 μm particle size, 2.1 × 100 mm). The chromatography parameters were set as follows: column temperature of 40 °C, flow rate of 0.3 mL/min, and injection volume of 10 μL. Gradient elution was conducted with two mobile phases: (A) water with 0.1% formic acid and (B) methanol with 0.1% formic acid. The separation began at 98:2 (A:B) and was adjusted to 0:100 (A:B) at 8 min. At 10 min, the gradient was reverted to 98:2 (A:B) and maintained until 12 min. A quadrupole-time-of-flight mass spectrometer (Q-TOF-MS) Xevo G2 from Waters Corporation (Milford, MA, USA) with an electrospray ionization (ESI) probe was coupled to the UPLC system. The following parameters were used: ESI+ (positive ionization mode); sensitivity (analyzer mode); capillary voltage of 2.8 kV; sampling cone voltage of 30 V; extraction cone voltage of 4 V; source temperature of 150 °C; cone gas flow rate of 40 L/h and desolvation gas flow rate of 600 L/h at a desolvation temperature of 400 °C. Data acquisition was performed in MSE mode, with both low and high collision energy (CE) in the collision cell, covering a mass range of m/z 50-1200. Leucine-Enkephalin ([M + H]+, m/z 556.2765) was used as the lock mass for real-time mass correction.

2.3. Statistical analysis

Statistical analysis of the results was performed using GraphPad Prism 8.02. Differences in mean scorings were analysed by multiple t-tests between bacterial species ($p < 0.05$).

3. Results and discussion

3.1. Materials characterization

In this work, we have selected to bio-based polymers, PHB and PLA to develop a new antimicrobial active packaging containing a volatile compound, BITC. included in cyclodextrins to improve the compatibility and processability of the materials enclosing the volatile compound. Both polymers chosen had similar barrier and mechanical properties, although having different glass transition temperatures, crystallinity degrees and degradation rates (Senila et al., 2025).

3.1.1. FT-IR analysis

Fig. 1 shows FT-IR analysis of films developed. In the case of PHB, a strong absorption band is seen at 1727 cm^{-1} corresponding to the C=O stretching vibration (Trakunjae et al., 2021). Small peaks are present at 2975 cm^{-1} and 2932 cm^{-1}, which correspond to methyl methylene vibration bond (Liau et al., 2014). The peak shown at 1453 cm^{-1} is related to the asymmetrical bending of CH_3, while at 1375 cm^{-1} another peak is shown related to the C-O-H bond (Liau et al., 2014). Additionally, a series of bands are present between 1000 cm^{-1} and 1300 cm^{-1}, with characteristic peaks at 1275 cm^{-1} and 1056 cm^{-1} corresponding to C-O stretching band (Ramezani et al., 2015; Trakunjae et al., 2021). In PLA films, the C=O stretching vibration peak appears at 1754 cm^{-1} (Fang et al., 2022), while the methyl stretching peak is seen at 3000 cm^{-1} and 2940 cm^{-1} (Kaynak & Meyva, 2014). Other PLA characteristic peaks appear at 1453 cm^{-1}, related to CH_3 group deformation, and three peaks at 1128 cm^{-1}, 1082 cm^{-1} and 1043 cm^{-1}, attributed to the symmetrical stretching of C-O-C (Fang et al., 2022; Kaynak & Meyva, 2014; Savaris et al., 2017).

Regarding the IC content in blends, only a small difference is seen at the peaks observed at 2933 cm^{-1} and 2922 cm^{-1}, which could be related to the β-CD C-H stretching vibration (Xu et al., 2020), although they can appear hidden by the methyl or methyl-methylene bond vibrations described above for each polymer. Apart from that, no other FT-IR peak can be attributed to the complex in either PHB or PLA films, perhaps due to the small concentration of IC added, up to 5 %.

3.1.2. XRD analysis

XRD diffractograms of developed films and pure β-CD are shown in Fig. 2. For PLA films, the pattern showed a mostly amorphous structure, with a broad maximum around $2\theta = 17°$, typically found in this polymer (Chu et al., 2017; Ramos et al., 2020). A different pattern is seen for PHB film samples, with various sharp peaks in the region of 10 – 30°, indicating a partial crystalline structure already described in literature (Chernozem et al., 2020; Pradhan et al., 2018). Contrarily to FT-IR analysis, XRD patterns of films clearly indicated the presence of the IC in active samples, showing a small peak around $2\theta = 11°$ in films with 2.5 and 5 % of IC, corresponding to the maximum peak found in the β-CD diffractogram. As expected, the peak increased with IC concentration, being higher for PHB_5IC and PLA_5IC than in PHB_2.5IC and PLA_2.5IC samples, respectively, and was not present in control samples (PHB_0IC and PLA_0IC). All of this confirmed an effective incorporation of the IC into the polymer matrixes.

3.1.3. DSC analysis

DSC results are shown in Table 1, which summarises the melting temperature T_m, fusion enthalpy (ΔH_m) and degree of crystallinity (χ_c) determined for each polymer and blend. Furthermore, an example of DSC profiles of pure polymers and blends is shown in Fig. 3

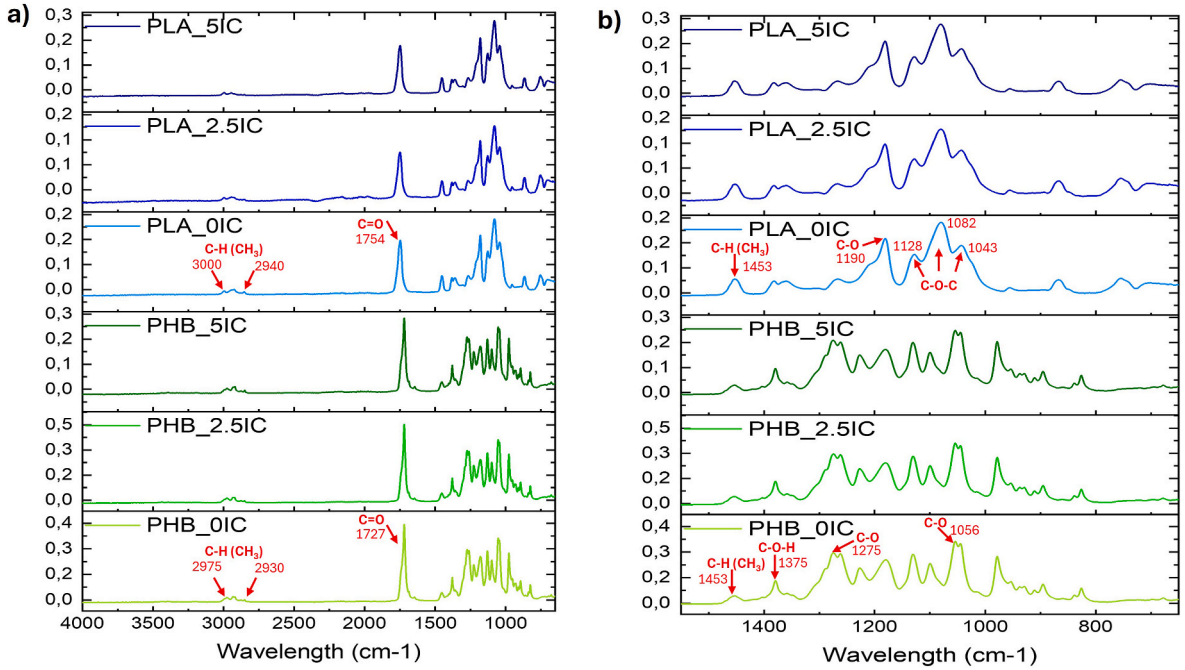

Fig. 1. FT-IR spectra of the developed films (PHB and PLA, with different inclusion complex (IC) concentrations: 0 %, 2.5 % and 5 %) in the range of a) 500 – 4000 cm^{-1} and b) 500 – 1500 cm^{-1}. Red arrows indicate significant peaks, and the corresponding functional groups are labelled.

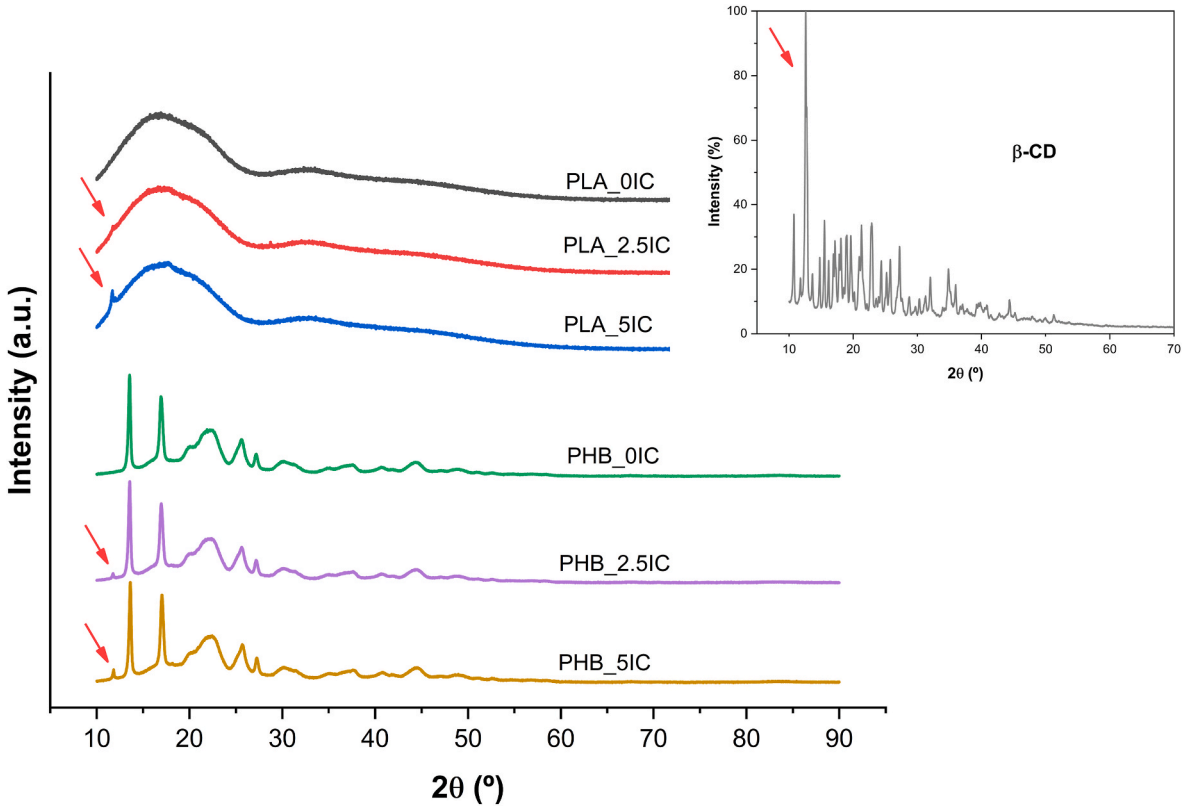

Fig. 2. XRD diffractograms of PHB and PLA films containing different concentrations of the inclusion complex (IC): 0 %, 2.5 % and 5 %. The top graph shows the XRD pattern of β-CD used in the IC formulation.

corresponding to the second heating cycle.

For PHB films, two melting temperature peaks can be seen at 137.2 and 148.9 °C, that can be the result of different inter-lamellae dimensions in the polymer structure (Garcia-Gonzalez et al., 2015). In the case of PLA, its melting temperature appears as a single peak at 150 °C, and its glass transition temperature appeared between 65 and 67 °C for all samples, which is in accordance to the data described by Greco and Ferrari (2021) and Monnier et al. (2017). Furthermore, a small peak

Table 1
Melting temperature (T_m), fusion enthalpy (ΔH_m) and degree of crystallization (χ_c) for each film obtained from DSC analysis.

	PHB						PLA		
Film	**T_{m1} (°C)**	**ΔH_{m1} (J/g)**	**χ_{c1} (%)**	**T_{m2} (°C)**	**ΔH_{m2} (J/g)**	**χ_{c2} (%)**	**T_m (°C)**	**ΔH_m (J/g)**	**χ_c (%)**
0IC	137.2	11.8	8.1	148.9	9.7	6.7	149.1	40.2	1.6
2.5IC	136.1	11.8	8.1	147.9	11.0	7.5	148.7	18.5	0.9
5IC	133.7	16.8	11.5	146.3	17.6	12.0	149.3	17.4	0.5

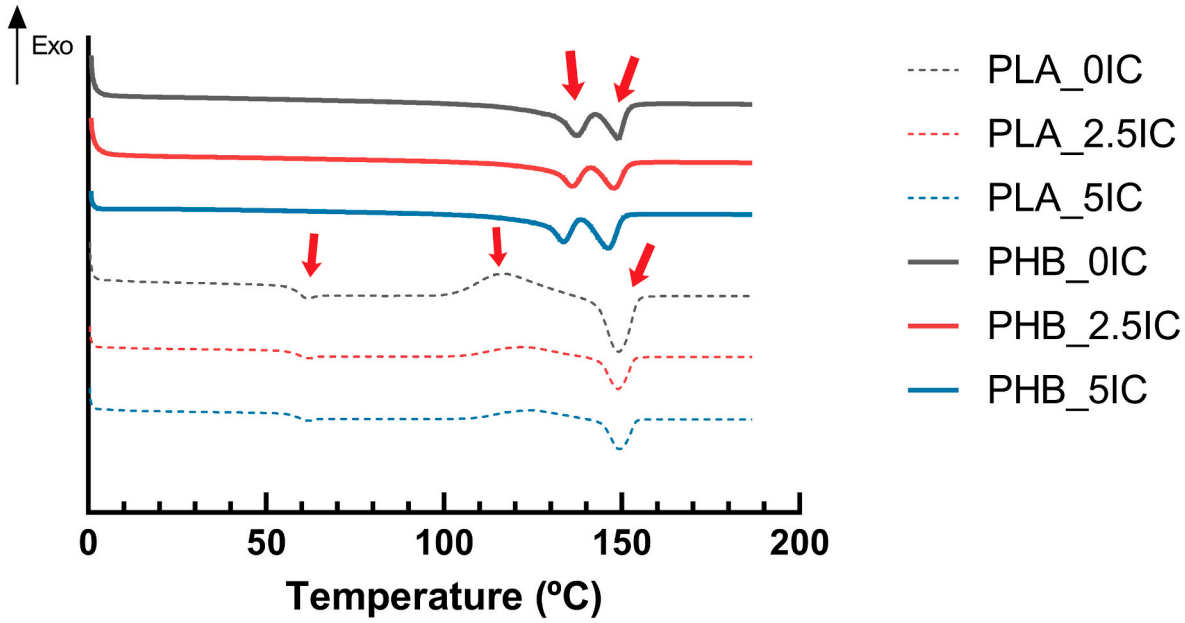

Fig. 3. Representative DSC thermograms of the developed films (PHB and PLA) containing different concentrations of the inclusion complex (IC): 0 %, 2.5 % and 5 %. Red arrows indicate significant thermal transitions.

regarding cold crystallization is seen around 120 °C, and it is probably related to a determined crystalline form (alpha or alpha'), which influences PLA melting behaviour (Tábi et al., 2016). The differences between the cold crystallization peak in PLA_0IC samples compared to PLA_2.5IC and PLA_5IC samples could be associated to the presence of different crystallization forms, the alpha form and the less ordered alpha' form (Tábi et al., 2016). Furthermore, an overall crystallization degree of less than 2 % is shown for all PLA samples, indicating that these films were amorphous. This is in accordance with those results explained by Drieskens et al. (2009), who developed PLA film samples by compression moulding and reported a degree of crystallinity of less than 2 %.

Regarding crystallinity degree in PHB samples, a slightly increase in its value can be seen in the case of PHB with IC, with an overall value of 23.5 % for PHB_5IC, when compared to 14.8 % for PHB without IC (PHB_0IC). This could be explained by the fact that the addition of the inclusion complex acted as a nucleating agent during extrusion, enhancing polymer crystallization. This role as a nucleating agents of other inclusion complexes, which are mainly composed by cyclodextrins, has already been stated by other studies (He & Inoue, 2003; Zhang et al., 2013). Besides, in the case of PHB_2.5IC, the crystallinity degree showed a despictable increase up to 15.6 % when compared to PHB alone, suggesting that at that concentration, the crystalline form of the polymer was slightly affected by IC. Based on available literature, this observed increase in crystallinity is expected to influence the mechanical properties of the developed films (El-Hadi et al., 2002; Majerczak et al., 2022), potentially enhancing their ductility and barrier performance (Iglesias-Montes et al., 2022, p. 3177). However, further studies are needed to confirm and quantify this effect.

3.1.4. TGA analysis

TGA results on films are depicted in Fig. 4. As seen for both polymers (PLA and PHB), degradation occurred in a single step. In the case of PLA, this degradation is mainly caused by the hydrolysis of the ester groups (Kangallı & Bayraktar, 2022), and it took place between 312 and 417 °C, with no major differences among samples. These results agree with those found by Kaavessina et al. (2015), who observed PLA degradation in a single step between 300 and 400 °C, with slight differences being attributable to different PLA blend and techniques used to prepare the samples. For PHB films, degradation occurred at lower temperatures, between 257 and 316 °C, due to cleavage of ester groups and crystalline regions (Pradhan et al., 2018). A small difference is seen in PHB_5IC with respect to other PHB samples, showing a small degradation step between 316 and 346 °C. We hypothesize this could be related to the β-CD present in the film, which in the case of PHB_5IC would be higher enough to yield a different TGA profile. For anhydrous β-CD, Hădărugă et al. (2019) reported a degradation temperature around 330 °C. Other authors (Sambasevam et al., 2013; Shown et al., 2010) who studied inclusion complexes formed with β-CD observed the degradation of the cyclodextrin between 300 and 367 °C, being in accordance with our results and thus, providing more evidence of IC incorporation in PHB_5IC samples.

3.1.5. Scanning electron microscopy analysis

Scanning electron micrographs of neat PHB and PLA films surface and cryo-fractured cross-sections stored at −20 ± 2 °C or at refrigerated temperature (4 ± 2 °C) were analysed by SEM at 8000X and 1000× magnifications, respectively (see Fig. 5). Surface images show clear differences between neat PHB and PLA surfaces, with PLA presenting a smooth surface (Fig. 5e and f) and PHB presenting some structures

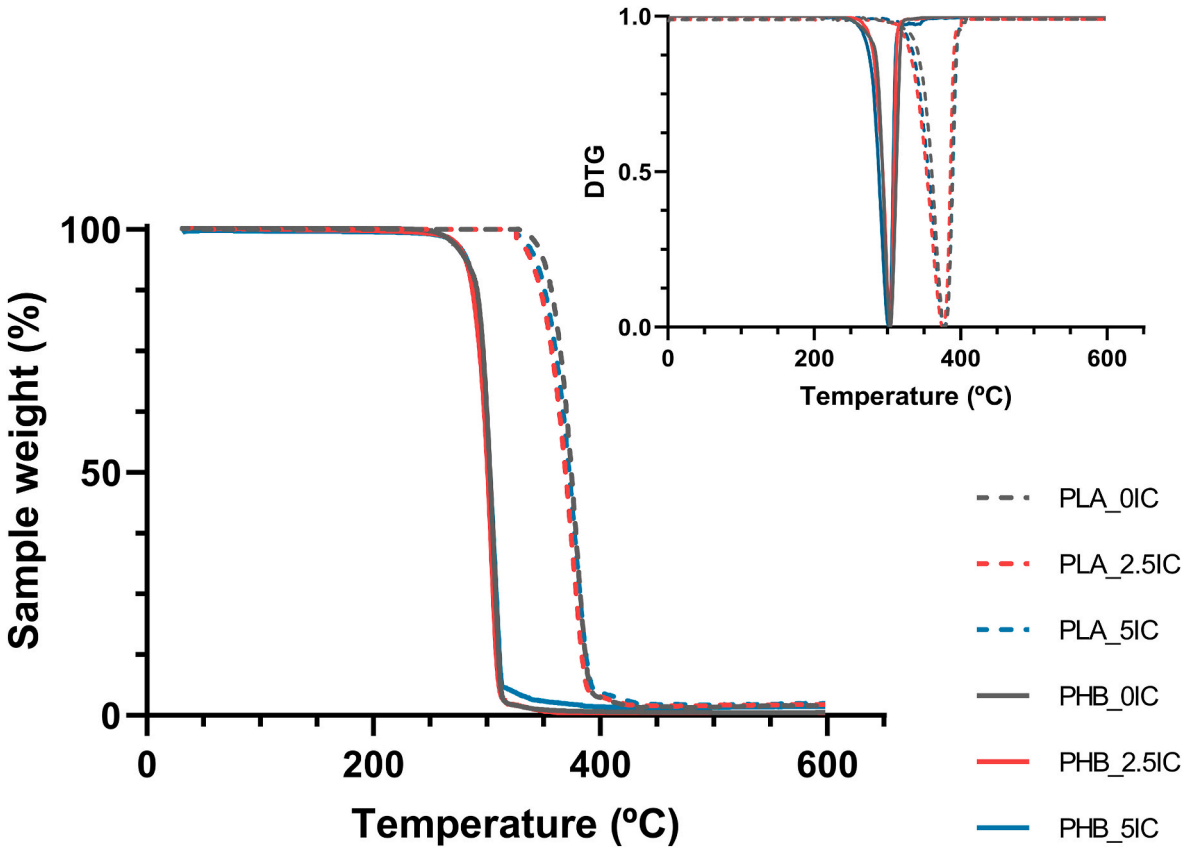

Fig. 4. TGA curves of prepared films (PHB and PLA) containing different inclusion complex (IC) concentrations: 0 %, 2.5 % and 5 %. The top graph shows the normalized derivative of TGA (DTG).

resembling crystals or flakes at the surface (Fig. 5a and b). Additionally, PHB surface did not present a porous surface as described by other authors (Park et al., 2022), which might be due to the manufacturing process and the additives contained in this commercial PHB polymer. Crystals are more abundant and more embedded on the surface of PHB films stored at refrigerated temperature (Fig. 5b) than at – 20 °C (Fig. 5a), which might indicate that the storage temperature could have some impact on crystal formation. This tendency can also be seen in the cryo-fractured cross-section images, as neat PHB films stored at 4 ± 2 °C (Fig. 5j) present a rougher surface than the ones stored at −20 ± 2 °C (Fig. 5i). With respect to neat PLA, no structural surface changes could be observed for films stored at refrigerated (Fig. 5e) and freezing temperatures (Fig. 5f). When it comes to the cross-section images, the same tendency can be seen, with a smooth surface being observed. Moreover, the cryo-fractured neat PLA cross-section images showed some thin and long fibrils spanning over the fractured zone. This finding has already been described by other authors (Eyholzer et al., 2012) that state that this might be due to a plastic fracture mechanism, which allows the material to yield long PLA fibrils (Eyholzer et al., 2012). Overall, PHB presents a rougher cryo-fractured surface when stored at refrigerated temperature while no visible structural alterations are visible for PLA films. Besides the crystals already present at the surface of the polymer, PHB films containing the IC showed bigger and rounder crystals with sizes of around 20 μm both at the surface (Fig. 5c and d) and within the polymer (Fig. 5k and l) that can be attributed to the IC itself, as the number of crystals increased with the increased in IC percentage within the PHB polymer (Fig. 5d–l). Within the polymer, most of the IC crystals can be found near the external sides of the polymer, mainly in PHB 5% IC. As can be seen from the cryo-fractured cross-section images, IC inclusion within the PHB matrix resulted in an increased roughness, with this roughness increasing with IC loading. Similar results have already been obtained by other authors developing PHB-cellulose composites (Schmidt et al., 2023). Contrarily to PHB, PLA did not present almost any IC crystals on the surface of the polymer, that remained smooth, despite the incorporation of the IC. However, when observing IC-containing PLA films cross-sections, it could be seen that the roughness increased in PLA films containing the IC, with no clear correlation between increased IC concentration and increased roughness. Some IC crystals could also be observed embedded within the PLA matrix, but of smaller size and at lower frequency than in PHB films. The addition of IC to the PLA matrix seemed to affect its plastic fracture mechanism, as the number of fibrils visualized in PLA 2.5% IC and 5% IC were gradually reduced. The higher number of crystals and their location near the external sides of the film might provide evidence for the increased antimicrobial activity of PHB films due to the increased ability of the IC to release BITC into the outside of the film.

3.2. *Determination of BITC content*

To further investigate whether the incorporation of IC in the polymer matrices affected BITC concentration, BITC was further determined in IC and in active films (Table 2). The amount of BITC included in the complex was found to be 110.3 ± 9.6 μg BITC per milligram of IC. In PHB films, BITC concentration was determined as 0.20 ± 0.02 and 0.39 ± 0.06 μg BITC/mg film for PHB_2.5IC and PHB_5IC, respectively. In the case of PHB_0IC, BITC was not detected, meaning that no cross-contamination occurred during film manufacturing. Considering that the mean weight of films was 18.5 ± 2 mg, the maximum amount of BITC included in the samples would be 45.5 – 55.1 μg for PHB_2.5IC and 91.0 – 110.2 μg for PHB_5IC. In that regard, the amount of BITC included in the films was much lower than expected, around 250 times lower than the theoretical expected value. These differences in the obtained value

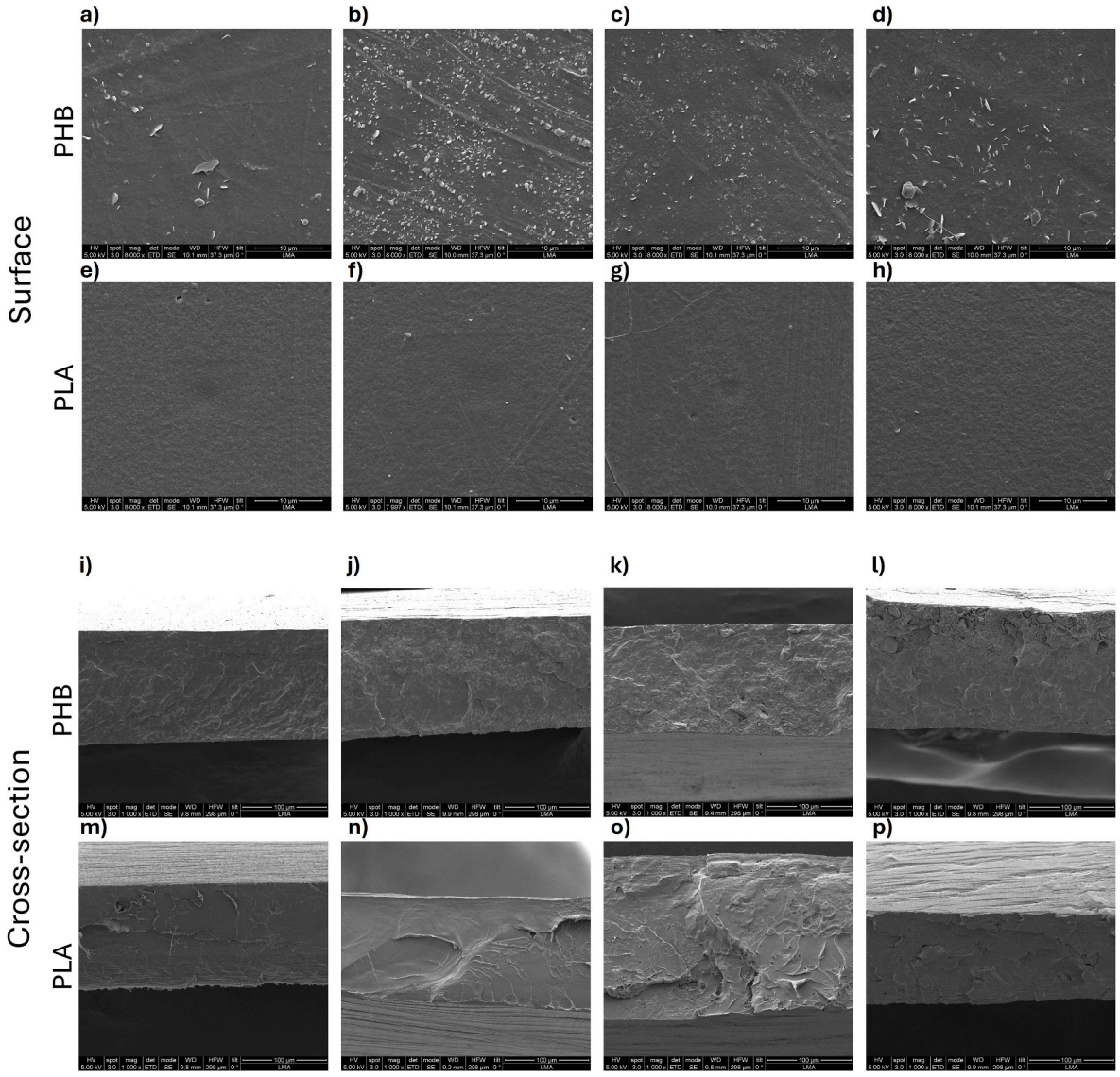

Fig. 5. SEM images of surface and cryo-fractured cross-sections of prepared PHB films with 0% IC(neat PHB, a, b, i, j), 2.5% IC (c, k) and 5% IC (d, l) and PLA films with 0% IC (neat PLA, e, f, m, n), 2.5% IC (g, o) and 5% IC (h, p). 0% IC (neat) films were stored at two different temperatures: PHB at −20 ± 2 °C (a, i), PHB at 4 ± 2 °C (b,j), and at −20 ± 2 °C (e, m), PHB at 4 ± 2 °C (j,n).

Table 2
BITC content (mean ± standard deviation) determined in the β-CD/BITC inclusion complex (IC) and in the developed films by GC-MS. In the case of developed films, expected (theoretical) BITC content is also shown.

Sample	Determined BITC (μg BITC/mg IC or film)	Expected BITC (μg BITC/mg film)
IC	110.33 ± 9.57	-
PHB_0IC	nd	nd
PHB_2.5IC	0.20 ± 0.02	50.3 ± 4.8
PHB_5IC	0.39 ± 0.06	100.6 ± 9.6
PLA_0IC	nd	nd
PLA_2.5IC	nd	50.3 ± 4.8
PLA_5IC	nd	100.6 ± 9.6

nd: not detected.

compared to the one expected related to the amount of antimicrobial added during synthesis of the IC may be attributed to the high temperatures reached during the extrusion and hot-pressing process (in the range of 150-175 °C for PHB), which may have enhanced BITC volatilization. In that scenario, it is suggested that not even the inclusion in the β-cyclodextrin cavity could prevent BITC loss due to volatilization. In fact, other authors working with another volatile compound (trans-2-hexenal have shown that there was a loss of 70 and 99% of compound after extrusion and after heat-press forming process, respectively (Joo et a., 2012).

For PLA films, it was not possible to BITC in any of the samples containing the IC, which could be attributed to the losses in volatile compound that occurred during processing, as the temperatures reached, in the range of 150-200 °C, were, at some points higher than in the case of PHB, or to some incompatibility between the polymer and BITC that hindered either its incorporation or release, hindering its recovery from the polymer through extraction. In fact, even the very different characteristics and properties of PLA and PHB could result in different release profiles, as PHB is known to degrade faster than PLA (Senila et al., 2025) and degradation rates seem to be correlated with compound release (Harting et al., 2019). Furthermore, although in the DSC results some slight differences between PLA_0IC and PLA_5IC samples have been noted in terms of crystallization, those could be related to the cyclodextrin itself and not to the BITC contained in the IC.

Our results showed that, although the polymers chosen had similar

properties, their behaviour in terms of performance when the same active antimicrobial agent is incorporated into the polymer matrix is different and should be considered when developing new active packaging materials.

3.3. Antibacterial activity

3.3.1. In liquid media

Results on antibacterial activity of BITC, synthesized IC and developed active films in liquid media are shown in Table 3. Regarding pure BITC, high antibacterial activity is shown against both *Campylobacter* strains, being slightly higher in the case of *C. jejuni*, with lower MIC and MBC values of 1 and 2 μg/mL, respectively, when compared to 4 and 2 μg/mL obtained for *C. coli*. These values are in line with those found by Dufour et al. (2012) against *C. jejuni* NTCT 1168 reference strain, who reported a MIC and MBC value of 1.25 μg/mL. To the best of our knowledge, BITC antibacterial activity against *C. coli* has not been reported in literature to date. The fact that *C. jejuni* was more sensitive to BITC (lower MIC and MBC values) than *C. coli* is in agreement with other authors that state that *C. coli* strains are usually more resistant to natural compounds and antibiotics than *C. jejuni* (Metreveli et al., 2022; Silva et al., 2015). The effect of BITC on other bacteria such as *Escherichia coli*, *Staphylococcus aureus* or *Salmonella enterica* was investigated by Clemente et al. (2017), who reported MIC values of 25, 25 and 50 μg/mL, respectively. In that regard, BITC showed lower MIC values for *Campylobacter* spp., which clearly testified to BITC potential use in controlling *Campylobacter* contamination.

With regard to IC activity against *Campylobacter* spp., MIC values of 18.1 and 9.1 μg/mL IC were found for *C. coli* and *C. jejuni* respectively, which correspond to 2 and 1 μg/mL BITC inside the complex. These results are consistent with the ones shown for pure BITC. Thus, the inclusion of BITC in the β-CD did not alter its antibacterial activity against both strains, proving that complexation with cyclodextrins could be an effective way of maintaining antibacterial properties while enhancing stability, as reported by Uppal et al. (2017).

Regarding the antibacterial activity of PHB and PLA films containing the IC, both active films exhibited highly different behaviour against *Campylobacter* spp. On the one hand, PHB active films with IC showed effective antibacterial properties even at the lowest IC content (inhibitory effects (IE) shown at 2.5% IC in the film; corresponding to 3.0-4.1 μg/mL theoretical BITC based on determined BITC concentration in IC). For *C. coli*, a higher IC concentration in the polymer was needed to achieve a bactericidal effect (BE, shown at 5 % IC; corresponding to 5.4-9.2 μg/mL theoretical BITC). Even so, the fact that *C. jejuni* is more susceptible than *C. coli* (inhibitory and bactericidal effects occurred at lower IC concentrations in the films for *C. jejuni*) to the active PHB films is consistent with the results on the antibacterial effect of pure BITC. On the other hand, PLA films containing the IC did not exhibit any antibacterial effect for both bacterial strains at any IC concentration tested, suggesting that IC incorporation in the polymer matrix did not occur in an effective way (not well dispersed) or that BITC could not be properly released from the PLA matrix, as already explained or even that all BITC was lost or degraded during film processing.

3.3.2. In solid media (vapour phase)

Fig. 6 shows the antibacterial activity of films in indirect contact (vapour phase) and an example of an inhibition halo produced by active films. PHB with IC active films produced high inhibition halos, with a diameter higher than 3 cm, for both *Campylobacter* strains. As expected, the antibacterial effect increased with IC content, being higher for PHB_5IC than for PHB_2.5IC due to a higher BITC concentration. These results indicate that the IC retained its antibacterial properties when included in the polymer matrix and that PHB_IC films were effective in inhibiting *Campylobacter* spp. growth. Similarly to liquid media tests, PLA_IC did not exhibit any antibacterial effect in vapour phase, proving once more that incorporation of IC in PLA matrix was not effective.

Although vapour phase and liquid media assays cannot be strictly compared due to differences in methodologies and diffusion profiles, in general both results are in accordance, with higher effect as the content of IC rises, and being *C. jejuni* more susceptible to the antimicrobial effect. To the extent of our knowledge, no other active material containing PHB and BITC into cyclodextrins has been developed. In 2016, Clemente et al. developed polypropylene labels containing 8 % pure BITC as antimicrobial and studied their effect in vapour phase against different moulds. In our case, we diminished the content of BITC in the material up to 0.2 % by using complexation with β-CD and still observed high antibacterial activity.

Furthermore, our results clearly illustrate that besides polymer processing conditions, the polymer matrix itself also plays a determinant role in the effectiveness of the active packaging material developed, because in this study, although the processing temperatures were similar for both PLA (150 - 200 °C) and PHB (150-170 °C), the resulting materials have very different behaviours when it comes to their BITC incorporation and/or release.

3.4. Migration assays on active films

Chemical safety of active films containing the maximum IC content evaluated (5% IC) was investigated through migration tests into food simulants. PLA films were not further investigated as they did not yield any antibacterial activity and therefore are not suitable to be used as active packaging materials.

When dealing with chemical compounds identified in migration tests, an important distinction is made based on the origin of the substance. If the compound has a known origin -for instance, it is intentionally added to enhance the polymer processing properties-it is classified as an IAS (*Intentionally Added Substance*). In contrast, when the origin of the compound is unknown, and could be the result of impurities or degradation processes, it is referred to as a NIAS (*Non-Intentionally Added Substance*) (Nerin, Alfaro, Aznar, & Domeño, 2013). Results on migration of volatile substances are shown in Table 4 while non-volatile substances are shown in Table 5.

Regarding volatile substances in both simulants, a small number of compounds were found. As expected for both simulants, BITC and the derivative benzyl isocyanate were found in all samples containing IC, whereas they were missing in samples without IC. Furthermore, lauryl and cetyl alcohols were found in all samples for both simulants. These compounds are commonly used as additives in different industries including the production of packaging materials where they are added as plasticizers (K. Groh et al., 2020; K. J. Groh et al., 2021). This might indicate that these compounds could be IAS, added to PHB to improve its mechanical properties during PHB manufacturing. Only one compound

Table 3
Antibacterial activity of pure BITC, IC and developed films against *Campylobacter* spp. Minimal Inhibitory Concentrations (MIC) and Minimal Bactericidal Concentrations (MBC) are expressed as μg/mL of BITC or IC solution. In the case of films of PLA or PHB, concentration of IC in the film at which inhibitory effect (IE) or bactericidal effect (BE) was observed are expressed as percentage of IC in the film.

Strain	BITC (μg/mL)		IC (μg/mL)		PHB + IC (% IC)		PLA + IC (% IC)	
	MIC	MBC	MIC	MBC	IE	BE	IE	BE
Campylobacter coli	2	4	18.1	72.0	≤2.5%	5%	>5%	>5%
Campylobacter jejuni	1	2	9.1	36.0	≤2.5%	2.5%	>5%	>5%

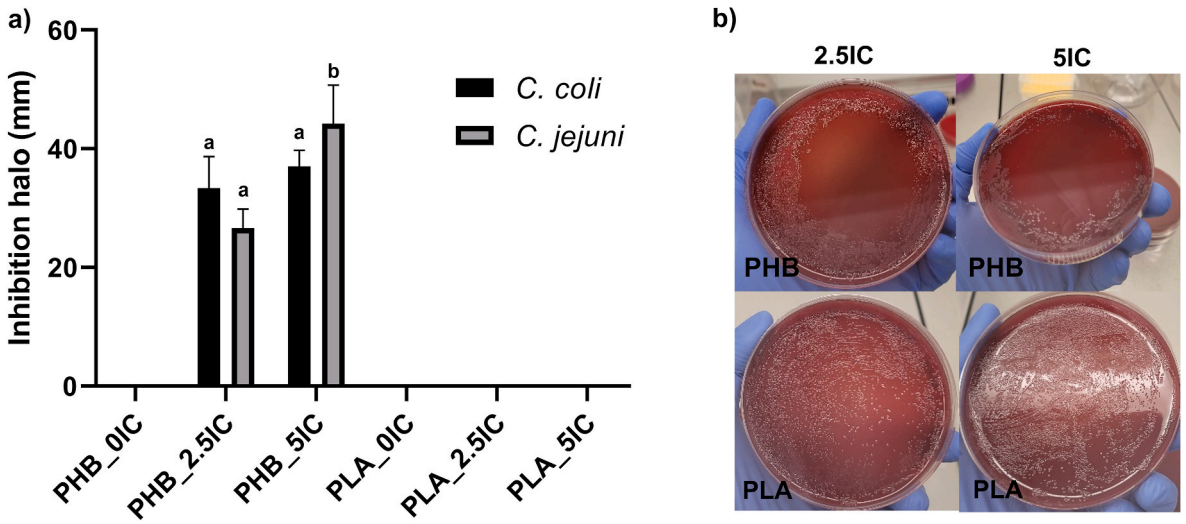

Fig. 6. Antibacterial effect of films in vapour phase. a) Results of inhibition halos (diameter mean and standard deviation expressed in mm). b) Example of inhibition halos produced by PHB and PLA with 2.5 % (2.5IC) and 5 % IC (5IC) in *C. jejuni* blood agar plate. Different letters for each day indicate a significant difference ($p < 0.05$) between species for each treatment.

Table 4
Volatile compounds and their retention times (t_R) found in migration tests in each simulant (simulant A - 10% ethanol; simulant D2 - 95% ethanol). 'X': found; '-': not found.

t_R	Molecular formula	Name	CAS	Simulant A		Simulant D2		Origin	Reference
				0IC	5IC	0IC	5IC		
9.780	C8H7NO	Benzyl isocyanate	3173-56-6	-	X	-	X	Oxidation of BITC by OH radicals	Lu et al. (2014)
13.459	C8H7NS	Benzyl isothiocyanate	622-78-6	-	X	-	X	Added during IC synthesis	-
14.903	C12H26O	Dodecanol (Lauryl alcohol)	36653-82-4	X	X	X	X	Plasticizer, dispersion agent	(K. Groh et al., 2020; K. J. Groh et al., 2021)
18.255	C16H34O	1-Hexadecanol (Cetyl alcohol)	36653-82-4	X	X	X	X	Plasticizer, dispersion agent	(K. Groh et al., 2020; K. J. Groh et al., 2021)
21.915				-	-	X	X		
22.660	C18H30O	Farnesyl acetone	762-29-8	-	-	X	X	Unknown; could be a by-product during bacterial PHB synthesis or as flavouring	Milker and Holtmann (2021)

Table 5
Non-volatile compounds and their retention times (t_R) found in migration tests in each food simulant (A: 10 % ethanol; D2: 95 % ethanol).'X': found; '-': not found.

t_R (min)	Mass (m/z)	Adduct	Molecular formula	Candidate name	CAS	0IC	5IC	Origin	Reference
Simulant A									
0.987	119.0700	$[M+H]^+$	$C_5H_{10}O_3$	3-hydroxipentanoic acid	10237-77-1	X	X	Sometimes used as copolymer with PHB to form PHBV	Ghanbarzadeh and Almasi (2013)
3.007	325.1125	$[M+H]^+$	$C_{12}H_{20}O_{10}$	β-Cyclodextrin	7585-39-9	-	X	Added during the synthesis of the IC	-
7.890	281.1009	$[M+Na]^+$	$C_{12}H_{18}O_6$	1,4 -Butanediol dimethacrylate	2082-81-7	X	X	Monomer for resins and crosslinking agent	(K. Groh et al., 2020; K. J. Groh et al., 2021)
8.300	367.1361	$[M+H]^+$	-	Unidentified		X	X		-
9.070	172.1695	$[M+H]^+$	$C_{10}H_{21}NO$	N, N-dimethyloctanamide	1118-92-9	X	X	Used as an emulsifier and solvent	United States Environmental Protection Agency (2020)
Simulant D2									
10.320	284.2956	[M+H]+	$C_{18}H_{37}NO$	Ocadecanamide	124-26-5	X	X	Additive; lubricant, adhesive, and anti-blocking agent	(K. Groh et al., 2020; K. J. Groh et al., 2021)
10.331	310.3122	[M+H]+	$C_{20}H_{39}NO$	cis-11- Eicosenamide	10436-08-5	X	X	Additive	(K. Groh et al., 2020; K. J. Groh et al., 2021)
10.624	338.3574	[M+H]+	$C_{22}H_{43}NO$	Erucamide	112-84-5	X	X	Additive; lubricant use, softener, adhesive	(K. Groh et al., 2020; K. J. Groh et al., 2021)
10.952	340.3664	[M+H]+	$C_{21}H_{45}N_3$	Guanidine, pentabutyl-	114591-53-6	X	X	Unknown, could be used as additive or surfactant	Vortman et al. (2024)

that was missing in simulant A was found in simulant D2, farnesyl acetone, due to its lipophilic character. The origin of this compound is unknown, although we hypothesize it could be related to the bacterial synthesis of PHB, as the derivarive β-farnesene has been found to be synthesized by the main PHB bacterial producer *Cupriavidus necator* (Milker & Holtmann, 2021), and therefore it could be classified as NIAS. Nevertheless, this compound is accepted as food flavouring agent by the EU (Commission Implementing Regulation (EU) No 872/2012).

In the case of non-volatile compounds, differences between both simulants were more pronounced. In simulant A, five substances were detected but only four of them were identified, while in simulant D2, four different substances were identified. Although the synthesis and manufacturing process of the commercial polymer cannot be known with certainty, the available literature indicates that most of the compounds identified in both simulants are IAS, used commonly as additives. A particular case is the compound identified as pentabutyl guanidine, only found in simulant B. In this case, only a single reference to this compound was found in literature, making it difficult to associate the compound with either an intentional or unintentional origin. Apart from that, the differences between the substances detected in each simulant are due to their hydrophilic or hydrophobic properties. For instance, in the case of simulant D2, the majority of the compounds detected were amides, while for simulant A, the detected compounds also included carboxylic acids and alcohols. β-CD was detected only in the case of the films containing the IC for simulant A due to its slightly hydrophilic nature (Yuan et al., 2009). Although it is known that β-CD-can be soluble in some organic solvents, namely some polar aprotic solvents (Hedges, 2009), this is not the case of ethanol, and that may explain why the cyclodextrin was not found in simulant D2 (95% ethanol).

As no other differences were detected between control and active film samples, we could hypothesize that all the compounds found in both types of samples, with the exception of BITC and β-CD, were IAS derived from the commercial polymer product, and added probably during polymer manufacturing as additives or processing helpers (Nerín, 2016). Apart from that, only the compounds forming the IC, BITC and β-CD, were found in the active samples. BITC is listed as food flavouring in the EU (Commission Implementing Regulation (EU) No 872/2012), while β-CD, β-cyclodextrin, only found in the aqueous simulant, is approved as additive, E 459, for all food categories excluding infant food (Commission Regulation (EU) No 1129/2011). When included in food contact materials, β-CD appears in the positive list of Commission Regulation 10/2011, although it does not have a specific migration limit (SML). However, when used as a carrier for food additives, flavourings, and nutrients, as in this case, β-CD is approved at concentrations up to 1000 mg/kg in the final food (Commission Regulation (EU) No 1129/2011). In our films, assuming that all β-CD incorporated in the polymer in the form of IC was to migrate into the food, the estimated amount –based on the standardized ratio of 6 dm^2 of packaging per kg of food (Commission Regulation (EU) 10/2011)– would range from 247.5 to 307.5 mg β-CD/kg of food for PHB_2.5IC, and from 495.0 to 615.0 mg β-CD/kg of food PHB_5IC, which are significantly below the established limit. All these data suggest that the incorporation of the IC in the polymer did not yield any additional compounds apart from β-CD and BITC, and thus, that the materials developed here could be feasible candidates to be marketed as active packaging materials. Nevertheless, more research is needed in terms of chemical risk assessment to determine whether all the compounds identified here comply with the migration limits established by the food contact materials regulation (Commission Regulation (EU) No 10/2011).

4. Conclusions

By means of complexation with β-CD and extrusion processing, we have successfully incorporated BITC into PHB polymer matrix and developed a novel biodegradable active material that proved effective against pathogenic gram-negative bacteria *Campylobacter jejuni* and *Campylobacter coli*. In the case of PLA, however, the incorporation and/or release of BITC appeared to be hindered, likely due to the processing temperatures applied during extrusion and hot pressing, or as a result of interactions with the PLA matrix itself. This observation underscores the considerable influence that polymer matrix has on the preservation of the active properties of the incorporated active agent, BITC, either by preventing its degradation or enabling its release. In any case, the results demonstrate the powerful anti-*Campylobacter* effect of PHB active films with an extremely low amount of BITC released, even when there is no direct contact between the film and the bacteria. Furthermore, the incorporation of the IC in the polymer did not produce any additional compound which could pose a chemical food safety risk, and most of the compounds could be identified as IAS, although more studies in terms of migration limit compliance must be performed. Moreover, these materials have been developed with industrial methods, such as extrusion and hot pressing, which suggests that they could be further used in food packaging applications such as labels or trays especially designed for poultry products where *Campylobacter* spp. is commonly found as a zoonotic agent, thus serving as a mean of controlling *Campylobacter* transmission through the consumption of this products and therefore the occurrence of campylobacteriosis in humans. Although migration studies bring the active packaging closer to real conditions, future research is needed to evaluate its effectiveness directly with food products.

CRediT authorship contribution statement

Laura Aguerri: Writing – review & editing, Writing – original draft, Visualization, Methodology, Investigation, Formal analysis, Data curation. **Estela Pérez-Bondía:** Investigation, Formal analysis. **Silvia Lóbez:** Resources, Investigation. **Frédéric Leonardi:** Writing – review & editing, Supervision, Resources. **Filomena Silva:** Writing – review & editing, Supervision, Resources, Funding acquisition, Conceptualization.

Declaration of competing interest

The authors declare that they have no known competing financial interests or personal relationships that could have appeared to influence the work reported in this paper.

Acknowledgements

This work has been funded by Grant TED2021-129138B-C21 funded by MICIU/AEI /10.13039/501100011033 and by the European Union NextGenerationEU/ PRTR. Grant PID2021-128089OB-I00 funded by MICIU/AEI /10.13039/501100011033 and by FEDER, UE.

Appendix A. Supplementary data

Supplementary data to this article can be found online at https://doi.org/10.1016/j.lwt.2026.119532.

Data availability

Data will be made available on request.

References

Abulreesh, H. H., Organji, S. R., Elbanna, K., Haridy Osman, G. E., Kareem Almalki, M. H., & Ahmad, I. (2017). Campylobacter in the environment: A major threat to public health. *Asian Pacific Journal of Tropical Disease, 7*(6), 374–384. https://doi.org/10.12980/apjtd.7.2017d6-392

Arrieta, M. P., Samper, M. D., López, J., & Jiménez, A. (2014). Combined effect of poly (hydroxybutyrate) and plasticizers on polylactic acid properties for film intended for food packaging. *Journal of Polymers and the Environment, 22*(4), 460–470. https://doi.org/10.1007/s10924-014-0654-y

Battegazzore, D., Bocchini, S., & Frache, A. (2011). Crystallization kinetics of poly(lactic acid)-talc composites. *Express Polymer Letters, 5*(10), 849–858. https://doi.org/10.3144/expresspolymlett.2011.84

Capelezzo, A. P., Mohr, L. C., Dalcanton, F., de Mello, J. M. M., & Fiori, M. A. (2018). β-Cyclodextrins as encapsulating agents of essential oils. In *Cyclodextrin-A versatile ingredient*. IntechOpen. https://doi.org/10.5772/intechopen.73568.

Chernozem, R. V., Guselnikova, O., Surmeneva, M. A., Postnikov, P. S., Abalymov, A. A., Parakhonskiy, B. V., De Roo, N., Skirtach, A. G., & Surmenev, R. A. (2020). Diazonium chemistry surface treatment of piezoelectric polyhydroxybutyrate

scaffolds for enhanced osteoblastic cell growth. *Applied Materials Today, 20*, Article 100758. https://doi.org/10.1016/j.apmt.2020.100758

Chu, Z., Zhao, T., Li, L., Fan, J., & Qin, Y. (2017). Characterization of antimicrobial poly (lactic acid)/nano-composite films with silver and zinc oxide nanoparticles. *Materials, 10*(6), 659. https://doi.org/10.3390/ma10060659

Clemente, I., Aznar, M., Salafranca, J., & Nerín, C. (2017). Raman spectroscopy, electronic microscopy and SPME-GC-MS to elucidate the mode of action of a new antimicrobial food packaging material. *Analytical and Bioanalytical Chemistry, 409*(4), 1037–1048. https://doi.org/10.1007/s00216-016-0022-y

Clinical and Laboratory Standards Institute (CLSI). (1999). *M26-A: Methods for determining bactericidal activity of antimicrobial agents*.

Clinical and Laboratory Standards Institute (CLSI). (2012). *M07-A9: Methods for dilution antimicrobial susceptibility tests for bacteria that grow aerobically* (12th ed.).

Clinical and Laboratory Standards Institute (CLSI). (2016). *M45: Methods for antimicrobial dilution and disk susceptibility testing of infrequently isolated or fastidious bacteria*.

Commission Implementing Regulation (EU). No 872/2012 of 1 October 2012 adopting the list of flavouring substances provided for by Regulation (EC) No 2232/96 of the European Parliament and of the Council, introducing it in Annex I to Regulation (EC) No 1334/2008 of the European Parliament and of the Council and repealing Commission Regulation (EC) No 1565/2000 and Commission Decision 1999/217/EC, applicable from 22/10/2012. http://data.europa.eu/eli/reg_impl/2012/872/oj.

Commission Regulation (EC). No 450/2009 of 29 May 2009 on active and intelligent materials and articles intended to come into contact with food. http://data.europa.eu/eli/reg/2009/450/oj.

Commission Regulation (EU). No 10/2011 of 14 January 2011 on plastic materials and articles intended to come into contact with food. http://data.europa.eu/eli/reg/2011/10/2025-03-16.

Commission Regulation (EU). No 1129/2011 of 11 November 2011 amending Annex II to Regulation (EC) no 1333/2008 of the European Parliament and of the Council by establishing a Union list of food additives. http://data.europa.eu/eli/reg/2011/1129/2013-11-21.

Drieskens, M., Peeters, R., Mullens, J., Franco, D., Lemstra, P. J., & Hristova-Bogaerds, D. G. (2009). Structure versus properties relationship of poly(lactic acid). I. Effect of crystallinity on barrier properties. *Journal of Polymer Science Part B: Polymer Physics, 47*(22), 2247–2258. https://doi.org/10.1002/polb.21822

Dufour, V., Alazzam, B., Ermel, G., Thepaut, M., Rossero, A., Tresse, O., & Baysse, C. (2012). Antimicrobial activities of isothiocyanates against Campylobacter jejuni isolates. *Frontiers in Cellular and Infection Microbiology, 2*. https://doi.org/10.3389/fcimb.2012.00053

El-Hadi, A., Schnabel, R., Straube, E., Müller, G., & Henning, S. (2002). Correlation between degree of crystallinity, morphology, glass temperature, mechanical properties and biodegradation of poly (3-hydroxyalkanoate) PHAs and their blends. *Polymer Testing, 21*(6), 665–674. https://doi.org/10.1016/S0142-9418(01)00142-8

European Food Safety Authority (EFSA) & European Centre for Disease Prevention and Control (ECDC). (2024). The European Union One Health 2023 Zoonoses report. *EFSA Journal, 22*(12). https://doi.org/10.2903/j.efsa.2024.9106

European Food Safety Authority (EFSA). (2024a). Campylobacter. https://www.efsa.europa.eu/en/topics/topic/campylobacter.

European Food Safety Authority (EFSA). (2024b). *Campylobacter story map*. ArcGIS StoryMaps. https://storymaps.arcgis.com/stories/37987745de6f47029e14cb57d61fe923.

Eyholzer, C., Tingaut, P., Zimmermann, T., & Oksman, K. (2012). Dispersion and reinforcing potential of carboxymethylated nanofibrillated cellulose powders modified with 1-Hexanol in extruded Poly(Lactic acid) (PLA) composites. *Journal of Polymers and the Environment, 20*(4), 1052–1062. https://doi.org/10.1007/S10924-012-0508-4/FIGURES/7

Fang, H., Zhang, L., Chen, A., & Wu, F. (2022). Improvement of mechanical property for PLA/TPU blend by adding PLA-TPU copolymers prepared via in situ ring-opening polymerization. *Polymers, 14*(8), 1530. https://doi.org/10.3390/polym14081530

Garcia-Garcia, D., Ferri, J. M., Boronat, T., Lopez-Martinez, J., & Balart, R. (2016). Processing and characterization of binary poly(hydroxybutyrate) (PHB) and poly (caprolactone) (PCL) blends with improved impact properties. *Polymer Bulletin, 73*(12), 3333–3350. https://doi.org/10.1007/s00289-016-1659-6

Garcia-Gonzalez, L., Mozumder, M. S. I., Dubreuil, M., Volcke, E. I. P., & De Wever, H. (2015). Sustainable autotrophic production of polyhydroxybutyrate (PHB) from CO_2 using a two-stage cultivation system. *Catalysis Today, 257*, 237–245. https://doi.org/10.1016/j.cattod.2014.05.025

Ghanbarzadeh, B., & Almasi, H. (2013). Biodegradable polymers. In R. Chamy (Ed.), *Biodegradation—life of science*. InTech. https://doi.org/10.5772/56230.

Gniewosz, M., Pobiega, K., Kraśniewska, K., Synowiec, A., Chaberek, M., & Galus, S. (2022). Characterization and antifungal activity of pullulan edible films enriched with propolis extract for active packaging. *Foods, 11*(15), 2319. https://doi.org/10.3390/foods11152319

Greco, A., & Ferrari, F. (2021). Thermal behavior of PLA plasticized by commercial and cardanol-derived plasticizers and the effect on the mechanical properties. *Journal of Thermal Analysis and Calorimetry, 146*(1), 131–141. https://doi.org/10.1007/s10973-020-10403-9

Groh, K. J., Geueke, B., Martin, O., Maffini, M., & Muncke, J. (2021). Overview of intentionally used food contact chemicals and their hazards. *Environment International, 150*, Article 106225. https://doi.org/10.1016/j.envint.2020.106225

Groh, K., Geueke, B., & Muncke, J. (2020). FCCdb: Food contact chemicals database. *Zenodo*. https://doi.org/10.5281/ZENODO.3240108 (Versión 5.0) Version 5.0. .

Hădărugă, N. G., Bandur, G. N., David, I., & Hădărugă, D. I. (2019). A review on thermal analyses of cyclodextrins and cyclodextrin complexes. *Environmental Chemistry Letters, 17*(1), 349–373. https://doi.org/10.1007/s10311-018-0806-8

Harting, R., Johnston, K., & Petersen, S. (2019). Correlating in vitro degradation and drug release kinetics of biopolymer-based drug delivery systems. *International Journal of Biobased Plastics, 1*(1), 8–21. https://doi.org/10.1080/24759651.2018.1563358

He, Y., & Inoue, Y. (2003). α-Cyclodextrin-enhanced crystallization of poly(3-hydroxybutyrate). *Biomacromolecules, 4*(6), 1865–1867. https://doi.org/10.1021/bm034260v

Hedges, A. (2009). Cyclodextrins: Properties and applications. In E. J. BeMiller, & R. Whistler (Eds.), *Starch* (3rd ed., pp. 833–851). Elsevier. https://doi.org/10.1016/S1082-0132(08)X0009-3.

Hoch, C. C., Shoykhet, M., Weiser, T., Griesbaum, L., Petry, J., Hachani, K., Multhoff, G., Bashiri Dezfouli, A., & Wollenberg, B. (2024). Isothiocyanates in medicine: A comprehensive review on phenylethyl-, allyl-, and benzyl-isothiocyanates. *Pharmacological Research, 201*, Article 107107. https://doi.org/10.1016/j.phrs.2024.107107

Iglesias-Montes, M. L., Soccio, M., Siracusa, V., Gazzano, M., Lotti, N., Cyras, V. P., & Manfredi, L. B. (2022). Chitin nanocomposite based on plasticized Poly(lactic acid)/Poly(3-hydroxybutyrate) (PLA/PHB) blends as fully biodegradable packaging materials. *Polymers, 14*(15), 3177. https://doi.org/10.3390/POLYM14153177. *Page 3177, 14*.

Jiang, J., Chen, X., Zhang, G.-L., Hao, H., Hou, H.-M., & Bi, J. (2022). Preparation of chitosan-cellulose-benzyl isothiocyanate nanocomposite film for food packaging applications. *Carbohydrate Polymers, 285*, Article 119234. https://doi.org/10.1016/j.carbpol.2022.119234

Joo, M. J., Merkel, C., Auras, R., & Almenar, E. (2012). Development and characterization of antimicrobial poly(l-lactic acid) containing trans-2-hexenal trapped in cyclodextrins. *International Journal of Food Microbiology, 153*(3), 297–305. https://doi.org/10.1016/J.IJFOODMICRO.2011.11.015

Kaavessina, M., Chafidz, A., Ali, I., & Al-Zahrani, S. M. (2015). Characterization of poly (lactic acid)/hydroxyapatite prepared by a solvent-blending technique: Viscoelasticity and in vitro hydrolytic degradation. *Journal of Elastomers & Plastics, 47*(8), 753–768. https://doi.org/10.1177/0095244314557973

Kangallı, E., & Bayraktar, E. (2022). Preparation and characterization of poly(lactic acid)/boron oxide nanocomposites: Thermal, mechanical, crystallization, and flammability properties. *Journal of Applied Polymer Science, 139*(28), Article e52521. https://doi.org/10.1002/app.52521

Kaynak, C., & Meyva, Y. (2014). Use of maleic anhydride compatibilization to improve toughness and other properties of polylactide blended with thermoplastic elastomers. *Polymers for Advanced Technologies, 25*(12), 1622–1632. https://doi.org/10.1002/pat.3415

Li, H., Ming, X., Wang, Z., Li, J., Liang, Y., Xu, D., Liu, Z., Hu, L., & Mo, H. (2022). Encapsulation of benzyl isothiocyanate with β-cyclodextrin using ultrasonication: Preparation, characterization, and antibacterial assay. *Foods, 11*(22), 3724. https://doi.org/10.3390/foods11223724

Liau, C. P., Bin Ahmad, M., Shameli, K., Yunus, W. M. Z. W., Ibrahim, N. A., Zainuddin, N., & Then, Y. Y. (2014). Preparation and characterization of polyhydroxybutyrate/polycaprolactone nanocomposites. *The Scientific World Journal, 2014*, 1–9. https://doi.org/10.1155/2014/572726

Lu, Z., Hebert, V. R., & Miller, G. C. (2014). Gas-phase reaction of methyl isothiocyanate and methyl isocyanate with hydroxyl radicals under static relative rate conditions. *Journal of Agricultural and Food Chemistry, 62*(8), 1792–1795. https://doi.org/10.1021/jf404526t

Luciano, F. B., & Holley, R. A. (2009). Enzymatic inhibition by allyl isothiocyanate and factors affecting its antimicrobial action against Escherichia coli O157:H7. *International Journal of Food Microbiology, 131*(2–3), 240–245. https://doi.org/10.1016/j.ijfoodmicro.2009.03.005

Ma, Y., Li, L., & Wang, Y. (2018). Development of PLA-PHB-based biodegradable active packaging and its application to salmon. *Packaging Technology and Science, 31*(11), 739–746. https://doi.org/10.1002/pts.2408

Majerczak, K., Wadkin-Snaith, D., Magueijo, V., Mulheran, P., Liggat, J., & Johnston, K. (2022). Polyhydroxybutyrate: A review of experimental and simulation studies of the effect of fillers on crystallinity and mechanical properties. *Polymer International, 71*(12), 1398–1408. https://doi.org/10.1002/pi.6402

Manso, S., Becerril, R., Nerín, C., & Gómez-Lus, R. (2015). Influence of pH and temperature variations on vapor phase action of an antifungal food packaging against five mold strains. *Food Control, 47*, 20–26. https://doi.org/10.1016/j.foodcont.2014.06.014

Manzoor, A., Khan, S., Dar, A. H., Pandey, V. K., Shams, R., Ahmad, S., Jeevarathinam, G., Kumar, M., Singh, P., & Pandiselvam, R. (2023). Recent insights into green antimicrobial packaging towards food safety reinforcement: A review. *Journal of Food Safety, 43*(4), Article e13046. https://doi.org/10.1111/jfs.13046

Metreveli, M., Bulia, S., Tevzadze, L., Tsanava, S., Zarske, M., Goenaga, J. C., Preuß, S., Lomidze, G., Koulouris, S., Imnadze, P., & Stingl, K. (2022). Comparison of antimicrobial susceptibility profiles of thermotolerant Campylobacter spp. isolated from human and poultry samples in Georgia (Caucasus). *Antibiotics, 11*(10), 1419. https://doi.org/10.3390/antibiotics11101419

Milker, S., & Holtmann, D. (2021). First time β-farnesene production by the versatile bacterium Cupriavidus necator. *Microbial Cell Factories, 20*(1), 89. https://doi.org/10.1186/s12934-021-01562-x

Mittal, M., Ahuja, S., Yadav, A., & Aggarwal, N. K. (2023). Development of poly (hydroxybutyrate) film incorporated with nano silica and clove essential oil intended for active packaging of brown bread. *International Journal of Biological Macromolecules, 233*, Article 123512. https://doi.org/10.1016/j.ijbiomac.2023.123512

Monnier, X., Saiter, A., & Dargent, E. (2017). Physical aging in PLA through standard DSC and fast scanning calorimetry investigations. *Thermochimica Acta, 648*, 13–22. https://doi.org/10.1016/j.tca.2016.12.006

Mukurumbira, A. R., Shellie, R. A., Keast, R., Palombo, E. A., & Jadhav, S. R. (2022). Encapsulation of essential oils and their application in antimicrobial active packaging. *Food Control, 136*, Article 108883. https://doi.org/10.1016/j.foodcont.2022.108883

Nerín, C. (2016). Migration analysis of compounds in food packaging. In M. P. Montero Garcia, M. C. Gómez-Guillén, M. E. López-Caballero, & G. V. Barbosa-Cánovas (Eds.), *Edible films and coatings* (1st ed.). CRC Press. https://doi.org/10.1201/9781315373713.

Nerin, C., Alfaro, P., Aznar, M., & Domeño, C. (2013). The challenge of identifying non-intentionally added substances from food packaging materials: A review. *Analytica Chimica Acta, 775*, 14–24. https://doi.org/10.1016/j.aca.2013.02.028

Nowicki, D., Krause, K., Karczewska, M., & Szalewska-Pałasz, A. (2021). Evaluation of the anti-shigellosis activity of dietary isothiocyanates in Galleria mellonella larvae. *Nutrients, 13*(11), 3967. https://doi.org/10.3390/nu13113967

Park, S. A., Yang, Y. H., & Choi, K. Y. (2022). One-pot production of thermostable PHB biodegradable polymer by co-producing bio-melanin pigment in engineered Escherichia coli. *Biomass Conversion and Biorefinery, 1*, 1–9. https://doi.org/10.1007/S13399-021-02222-1/FIGURES/6

Perinelli, D. R., Palmieri, G. F., Cespi, M., & Bonacucina, G. (2020). Encapsulation of flavours and fragrances into polymeric capsules and cyclodextrins inclusion complexes: An update. *Molecules, 25*(24), 5878. https://doi.org/10.3390/molecules25245878

Petrovic, G. M., Stojanovi, G. S., & Radulovi, N. S. (2010). Encapsulation of cinnamon oil in β-cyclodextrin. *Journal of Medicinal Plants Research, 4*(14), 1382–1390.

Pradhan, S., Dikshit, P. K., & Moholkar, V. S. (2018). Production, ultrasonic extraction, and characterization of poly (3-hydroxybutyrate) (PHB) using *Bacillus megaterium* and *Cupriavidus necator*. *Polymers for Advanced Technologies, 29*(8), 2392–2400. https://doi.org/10.1002/pat.4351

Ramezani, M., Amoozegar, M. A., & Ventosa, A. (2015). Screening and comparative assay of poly-hydroxyalkanoates produced by bacteria isolated from the Gavkhooni Wetland in Iran and evaluation of poly-β-hydroxybutyrate production by halotolerant bacterium Oceanimonas sp. GK1. *Annals of Microbiology, 65*(1), 517–526. https://doi.org/10.1007/s13213-014-0887-y

Ramos, M., Beltran, A., Fortunati, E., Peltzer, M., Cristofaro, F., Visai, L., Valente, A. J. M., Jiménez, A., Kenny, J. M., & Garrigós, M. C. (2020). Controlled release of thymol from poly (lactic acid)-based silver nanocomposite films with antibacterial and antioxidant activity. *Antioxidants, 9*(5), 395. https://doi.org/10.3390/antiox9050395

Rusková, M., Opálková Šišková, A., Mosnáčková, K., Gago, C., Guerreiro, A., Bučková, M., Puškárová, A., Pangallo, D., & Antunes, M. D. (2023). Biodegradable active packaging enriched with essential oils for enhancing the shelf life of strawberries. *Antioxidants, 12*(3), 755. https://doi.org/10.3390/antiox12030755

Sambasevam, K., Mohamad, S., Sarih, N., & Ismail, N. (2013). Synthesis and characterization of the inclusion complex of β-cyclodextrin and azomethine. *International Journal of Molecular Sciences, 14*(2), 3671–3682. https://doi.org/10.3390/ijms14023671

Savaris, M., Braga, G. L., dos Santos, V., Carvalho, G. A., Falavigna, A., Machado, D. C., Viezzer, C., & Brandalise, R. N. (2017). Biocompatibility assessment of poly (lactic acid) films after sterilization with ethylene oxide in histological study in vivo with wistar rats and cellular adhesion of fibroblasts in vitro. *International Journal of Polymer Science, 2017*(1), Article 7158650. https://doi.org/10.1155/2017/7158650

Schmidt, A., Bittmann-Hennes, B., Montero, B., Wetzel, B., & Barral, L. (2023). Green bionanocomposites based on polyhydroxybutyrate and filled with cellulose nanocrystals: Melting processing and characterization. *Journal of Polymers and the Environment, 31*(11), 4801–4816. https://doi.org/10.1007/S10924-023-02835-9/FIGURES/9

Senila, L., Kovacs, E., & Senila, M. (2025). A review of polylactic acid (PLA) and Poly(3-hydroxybutyrate) (PHB) as bio-sourced polymers for membrane production applications. *Membranes, 15*(7), 210. https://doi.org/10.3390/MEMBRANES15070210

Shown, I., Banerjee, S., Ramchandran, A. V., Geckeler, K. E., & Murthy, C. N. (2010). Synthesis of cyclodextrin and sugar-based oligomers for the efavirenz drug delivery. *Macromolecular Symposia, 287*(1), 51–59. https://doi.org/10.1002/masy.201050108

Silva, F., Domingues, F. C., & Nerín, C. (2018). Control microbial growth on fresh chicken meat using pinosylvin inclusion complexes based packaging absorbent pads. *Lebensmittel-Wissenschaft & Technologie, 89*, 148–154. https://doi.org/10.1016/j.lwt.2017.10.043

Silva, F., Nerín, C., & Domingues, F. C. (2015). Stilbene phytoallexins inclusion complexes: A natural-based strategy to control foodborne pathogen Campylobacter. *Food Control, 54*, 66–73. https://doi.org/10.1016/j.foodcont.2015.01.039

Sofi, S. A., Singh, J., Rafiq, S., Ashraf, U., Dar, B. N., & Nayik, G. A. (2018). A comprehensive review on antimicrobial packaging and its use in food packaging. *Current Nutrition & Food Science, 14*(4), 305–312. https://doi.org/10.2174/1573401313666170609095732

Sun, Y., Wang, Y., Xu, Y., Chen, T., Li, B., Zhang, Z., & Tian, S. (2021). Application and mechanism of benzyl-isothiocyanate, a natural antimicrobial agent from cruciferous vegetables, in controlling postharvest decay of strawberry. *Postharvest Biology and Technology, 180*, Article 111604. https://doi.org/10.1016/j.postharvbio.2021.111604

Tábi, T., Hajba, S., & Kovács, J. G. (2016). Effect of crystalline forms (α′ and α) of poly (lactic acid) on its mechanical, thermo-mechanical, heat deflection temperature and creep properties. *European Polymer Journal, 82*, 232–243. https://doi.org/10.1016/j.eurpolymj.2016.07.024

Taktak, I., Mansouri, A., Guerfali, M., Ayadi, I., Souissi, S., Gargouri, A., Etoh, M.-A., & Elloumi, A. (2024). Active bio composites films based on PLA/olive wood flour (Olea europaea L.)/cinnamon essential oil. *Polymer Bulletin, 81*(1), 719–737. https://doi.org/10.1007/s00289-023-04737-1

Trakunjae, C., Boondaeng, A., Apiwatanapiwat, W., Kosugi, A., Arai, T., Sudesh, K., & Vaithanomsat, P. (2021). Enhanced polyhydroxybutyrate (PHB) production by newly isolated rare actinomycetes Rhodococcus sp. Strain BSRT1-1 using response surface methodology. *Scientific Reports, 11*(1), 1896. https://doi.org/10.1038/s41598-021-81386-2

United States Environmental Protection Agency. (2020). Chemical data reporting data [Other Policies and Guidance] https://www.epa.gov/chemical-data-reporting/access-chemical-data-reporting-data.

Uppal, S., Kaur, K., Kumar, R., Kahlon, N. K., Singh, R., & Mehta, S. K. (2017). Encompassment of benzyl isothiocyanate in cyclodextrin using ultrasonication methodology to enhance its stability for biological applications. *Ultrasonics Sonochemistry, 39*, 25–33. https://doi.org/10.1016/j.ultsonch.2017.04.007

Vortman, M., Lemeshko, V., & Shevchenko, V. (2024). Guanidinium-containing oligomeric cationic protonic ionic liquid. *Reports of the National Academy of Sciences of Ukraine, 12*, 75–82. https://doi.org/10.15407/dopovidi2019.12.075

Waddell, W. J., Cohen, S. M., Feron, V. J., Goodman, J. I., Marnett, L. J., Portoghese, P. S., Reitjiens, I. M. C. M., Smith, R. L., Adams, T. B., Lucas Gavin, C., McGowen, M. M., & Williams, M. C. (2007). GRAS flavoring substances 23. *Food Technology, 61*(8), 22–61.

Wilson, A. E., Bergaentzlé, M., Bindler, F., Marchioni, E., Lintz, A., & Ennahar, S. (2013). In vitro efficacies of various isothiocyanates from cruciferous vegetables as antimicrobial agents against foodborne pathogens and spoilage bacteria. *Food Control, 30*(1), 318–324. https://doi.org/10.1016/j.foodcont.2012.07.031

World Health Organization (WHO). (2020). Campylobacter. https://www.who.int/news-room/fact-sheets/detail/campylobacter.

Wu, H., Ao, X., Liu, J., Zhu, J., Bi, J., Hou, H., Hao, H., & Zhang, G. (2022). A bioactive chitosan−based film enriched with benzyl isothiocyanate/α−cyclodextrin inclusion complex and its application for beef preservation. *Foods, 11*(17), 2687. https://doi.org/10.3390/foods11172687

Xiao, Z., Zhang, Y., Niu, Y., Ke, Q., & Kou, X. (2021). Cyclodextrins as carriers for volatile aroma compounds: A review. *Carbohydrate Polymers, 269*, Article 118292. https://doi.org/10.1016/j.carbpol.2021.118292

Xu, R., Lin, X., Xu, J., & Lei, C. (2020). Controlling the water absorption and improving the high C-rate stability: A coated Li-ion battery separator using β-cyclodextrin as binder. *Ionics, 26*(7), 3359–3365. https://doi.org/10.1007/s11581-020-03449-0

Yadav, K., Dhankhar, J., & Kundu, P. (2022). Isothiocyanates – A review of their health benefits and potential food applications. *Current Research in Nutrition and Food Science Journal, 10*(2), 476–502. https://doi.org/10.12944/CRNFSJ.10.2.6

Yuan, H.-N., Yao, S.-J., Shen, L.-Q., & Mao, J.-W. (2009). Preparation and characterization of inclusion complexes of β-cyclodextrin−BITC and β-cyclodextrin−PEITC. *Industrial & Engineering Chemistry Research, 48*(10), 5070–5078. https://doi.org/10.1021/ie8015329

Zhang, R., Wang, Y., Wang, K., Zheng, G., Li, Q., & Shen, C. (2013). Crystallization of poly(lactic acid) accelerated by cyclodextrin complex as nucleating agent. *Polymer Bulletin, 70*(1), 195–206. https://doi.org/10.1007/s00289-012-0814-y

Zhuikova, Y., Zhuikov, V., & Varlamov, V. (2022). Biocomposite materials based on Poly (3-hydroxybutyrate) and chitosan: A review. *Polymers, 14*(24), 5549. https://doi.org/10.3390/polym14245549